



Published in final edited form as:

J Biol Chem. 2007 March 30; 282(13): 9768–9776.

Nuclear Pregnane X Receptor Cross-talk with FoxA2 to Mediate Drug-induced Regulation of Lipid Metabolism in Fasting Mouse Liver

Kouichi Nakamura, Rick Moore, Masahiko Negishi^{*}, and Tatsuya Sueyoshi

Pharmacogenetics Section, Laboratory of Reproductive and Developmental Toxicology, National Institute of Environmental Health Science, National Institute of Health, Research Triangle Park, NC 27709

Abstract

Upon drug activation, the nuclear pregnane X receptor (PXR) regulates not only hepatic drug but also energy metabolism. Using *Pxr*^{-/-} mice, we have now investigated the PXR-mediated repression of lipid metabolism in the fasting livers. Treatment with PXR activator pregnenolone 16 α -carbonitrile (PCN) down-regulated the mRNA levels of carnitine palmitoyltransferase 1 A (CPT1A, in β -oxidation) and mitochondrial 3-hydroxy-3-methylglutarate CoA synthase 2 (HMGCS2, in ketogenesis) in the wild type (*Pxr*^{+/+}) mice only. In contrast, the stearoyl-Coenzyme A desaturase 1 (SCD1, in lipogenesis) mRNA was up-regulated in the PCN-treated *Pxr*^{+/+} mice. Reflecting these up- and down-regulations and consistent with decreased energy metabolism, the levels of hepatic triglycerides and of serum 3-hydroxybutyrate were increased and decreased, respectively in the PCN-treated *Pxr*^{+/+} mice. Using gel shift, GST pull down and cell-based reporter assays, we then examined whether PXR could cross talk with the insulin response forkhead factor FoxA2 to repress the transcription of the *Cpt1a* and *Hmgcs2* genes, since FoxA2 activates these genes in fasting liver. PXR directly bound to FoxA2 and repressed its activation of the *Cpt1a* and *Hmgcs2* promoters. Moreover, ChIP assays showed that PCN treatment attenuated the binding of FoxA2 to these promoters in fasting *Pxr*^{+/+} but not *Pxr*^{-/-} mice. These results are consistent with the conclusion that PCN-activated PXR represses FoxA2-mediated transcription of *Cpt1a* and *Hmgcs2* genes in fasting liver.

The nuclear receptors CAR (NR1I3) and PXR (NR1I2) were first characterized as xenobiotic-sensing transcription factors (1-3) coordinately inducing the expression of hepatic genes that encode various enzymes and proteins involved in drug metabolism and excretion (4-8). Those enzymes include cytochromes P450 (9,10), UDP-glucuronosyltransferases (11-13), sulfotransferases (14) and drug transporters (15). However, our studies have now shown CAR represses the genes encoding enzymes such as phosphoenolpyruvate carboxykinase 1 (PEPCK1), carnitine palmitoyltransferase 1A (CPT1A) and enoyl-CoA isomerase (ECI) (16, 17). It is also known that PXR can regulate the expression of the *Pepck1* and *Cpt1a* genes (17,18). Thus, in addition to drug metabolism, these nuclear receptors modulate hepatic energy metabolism, glucogenogenesis and fatty acid oxidation (6). The molecular mechanism of how CAR and PXR mediate the drug-induced repression of energy metabolism is currently a strong research interest.

The liver is the major organ that metabolizes lipids to produce energy sources. Through β -oxidation and ketogenesis the liver supplies the major energy sources ketone bodies

Address correspondence to: Dr. Masahiko Negishi, Pharmacogenetics Section, Laboratory of Reproductive and Developmental Toxicology, National Institute of Environmental Health Science, National Institute of Health, Research Triangle Park, NC 27709, Tel. 919-541-2404; Fax 919-541-0696; E-mail: negishi@niehs.nih.gov.

(acetoacetate and 3-hydroxybutyrate) to the extra-hepatic tissues and organs when blood glucose levels are low after fasting and prolonged exercise (19-22). The genes such as *Cpt1a* and *mitochondrial 3-hydroxy-3-methylglutarate CoA synthase 2 (Hmgcs2)* are activated to increase the supply of ketone bodies (23,24). Recently, FoxA2, a winged -helix/forkhead transcription factor, is found to be the key regulatory factor that activates these genes in fasting mouse liver (25). Insulin decreases lipid metabolism by inactivating the transcription factor FoxA2 to control energy metabolism (26,27). Treatment with drugs such as phenobarbital (PB) can modulate lipid metabolism in an insulin independent manner by changing the expression of many genes under control of insulin signaling cascade (28), suggesting that there may be cross talk between the xenobiotic-sensing transcription and insulin regulated transcription factors. Recently, the molecular mechanism by which both CAR and PXR decrease gluconeogenesis was elucidated. Both receptors directly bind to FoxO1, preventing its interaction with the insulin response sequence (IRS) and repressing the FoxO1-mediated activation of IRS-bearing genes such as *Pepck1* (17). However, the molecular mechanism by which CAR and PXR represses lipid metabolism remains unexplored.

We have investigated the molecular mechanism of PXR-mediated regulation of hepatic lipid metabolism in fasting mouse. *Pxr*^{-/-} mice were used to demonstrate that the activation of PXR down-regulated the key enzymes in β -oxidation and ketogenesis, CPT1A and HMGCS2 respectively, while up-regulating stearoyl-Coenzyme A desaturase 1 (SCD1), the key enzyme in lipogenesis. By cloning and characterizing the promoters of the mouse *Cpt1a* and *Hmgcs2* genes, we deciphered the repression mechanism by PXR of FoxA2-mediated transcription of these genes. Here we present experimental considerations to propose the regulatory mechanism by which the drug activation of PXR can result in decreased energy metabolism by up-regulating lipogenesis and by down-regulating β -oxidation and ketogenesis in fasting mouse liver.

Experimental procedures

Materials

Dimethyl sulfoxide (DMSO) and pregnenolone 16 α -carbonitrile (PCN) were purchased from Sigma-Aldrich. The plasmids pGL3-basic, pBIND and pACT were obtained from Promega. Restriction endonucleases and DNA-modifying enzymes were purchased from New England Biolabs, Inc.

Plasmid construction

pGem1/rat FOXA2/Hnf3 β and 6xFoxA TATA-Luc were kindly provided by Robert H. Costa (29,30). In all plasmid, m and h denote mouse and human, respectively. The following plasmids were described previously: pCMX/hRXR(1), pcDNA/mPXR(31), and pcDNA3.1/mPXR Δ AF2-V5-His (31). Rat FoxA2 coding DNA was amplified using proper primer sets with pGem1/rat Hnf3 β /FoxA2 as the template and subcloned into pcDNA3.1/V5-His-Topo (Invitrogen), pGEX4T-1 (Amersham Biosciences), and pACT to generate pcDNA3.1/FoxA2, pGEX/FoxA2 and pACT/FoxA2, respectively. pBind/mPXR were constructed by cloning of mPXR into pBIND. The following deletion mutants were also constructed based on the previous report (29): pGEX/FoxA2 7-94, pGEX/FoxA2 144-279, pGEX/FoxA2 361-458, pcDNA3.1/mPXR-LBD-V5-His (amino acid 141 to 431), pcDNA3.1/mPXR-DBD-V5-His (amino acid 1 to 104). Reporter plasmids pGL3/CPT1a-2.4k and pGL3/HMGCS2 -3.0k were constructed using PCR amplified *Cpt1a* promoter (-2432 to +1) and *Hmgcs2* promoter (-2984 to +40) from mouse genomic DNA, respectively. Primers used for these cloning are 5'-GCATATCTCGAGATCACTCAAGCTGGCCTCAAACCTTGTGG-3' and 5'-TTCTTGAAGCTTCTTGGAGGAGGGGCAAGAGATGGCTTTGAG for *Cpt1a* and 5'-GCATATGGTACCTCTACTACAATAAGACATGGCAGAGG-3' and 5'-

CGGCTACTCGAGATCAACAGAAAGCCAGCAGTCCACAG-3' for *Hmgcs2*. The amplified DNA fragments are cloned into pGL3 basic at *XhoI-HindIII* and *KpnI-XhoI* sites, respectively, utilizing the recognition sequences incorporated in the primers as indicated by underlines.

Cell culture and transfection

HepG2 and Huh7 cells were cultured in minimum essential medium supplemented with 10% fetal bovine serum, 2 mM L-glutamine, 100 U/ml penicillin, and 100 µg/ml streptomycin in an atmosphere of 5% CO₂ at 37°C. The cells on 24-wells plates were transfected with Fugene 6 (Roche Diagnostics) according to the manufacture's instruction. Twenty four h after transfection, cells were treated with drug in the media without FBS for an additional 24 h before harvest. Luciferase activity was measured using the Dual-Luciferase reporter assay system (Promega) and normalized against Renilla reniformis luciferase activity from pRL-CMV (10 ng/well) (Promega). The experiments were carried out in triplicate, and the results are expressed as the mean ± standard deviation.

Mammalian two-hybrid assay

Mammalian two-hybrid assay was performed using CheckMate Mammalian Two Hybrid System (Promega) according to the manufacturer's instructions. Expression plasmids for GAL4 DNA binding domain (pBIND) fusion protein and VP16 (pACT) fusion protein were cotransfected into HepG2 cells with pG5Luc reporter plasmid, and luciferase activity was determined as described above.

GST pull-down

Glutathione S-transferase (GST) fusion proteins, GST-FoxA2, GST-FoxA2 7-94, GST-FoxA2 144-279 and GST-FoxA2 361-458 were expressed in *Escherichia coli* strain BL21 cells and were purified with glutathione-Sepharose 4B (Amersham Biosciences). mPXR, mPXR DBD, mPXR LBD and mPXR ΔAF2 were labeled with [³⁵S] methionine using the TNT T7 quick-coupled transcription/translation system (Promega). GST-FoxA2 was incubated with ³⁵S-labeled mPXR or the mutants, and then GST pull down procedure was performed as previously reported (32). Bound proteins were detected by autoradiography after SDS-PAGE separation.

Gel shifts

PXR, RXR and FoxA2 proteins were produced by *in vitro* translation using appropriate expression plasmid and a TNT T7 quick-coupled transcription/translation system. For the probes, double-stranded oligonucleotides containing a FoxA2 binding site of hIGFBP-1 promoter at the position -124 to -96 (5'-GATCCACTAGCAAACAAACTTATTTGAACACGATC-3') (33), the putative FoxA2 binding sites within *Cpt1a* promoter, C1 at the position -1910 to -1886 (5'-GATCAAGCTAAACAGGCATGATC-3'), C2 at the position -1823 to -1809 (5'-GATCCATATAAATATGCAGGATC-3'), C3 at the position -1733 to -1719 (5'-GATCATACCTATTGGTTTTGATC-3'), the binding sites within *Hmgcs2* promoter, H1 at the position -179 to -162 (5'-GATCAAGGCCAACAATGAAGATC-3'), and H2 at the position -112 to -98 (5'-GATCCATGATGTTTTCTTGATC-3') were labeled with [α -³²P] dATP and DNA polymerase Klenow fragment (New England Biolabs). The underlined sequences indicate additional sequences for filled in by Klenow fragment. Gel shift assay were carried out as described previously (1).

Animal treatments

All animals were housed in a room maintained at 22°C with a 12:12-h light-dark cycle (7:00 AM to 7:00 PM). Mice were fed ad libitum with NIH-31 Open Formula Autoclavable diet (Zeigler). PXR wild type (*Pxr*^{+/+}) or null (*Pxr*^{-/-}) mice (10 weeks old) obtained from Jeff L. Staudinger were randomly divided into two groups and mice were intraperitoneally treated with PCN (20 mg/kg of body weight) or vehicle only (DMSO). After injection, mice (four mice per group) were fasted with food withdrawn but drinking water ad libitum until sacrificed. All animal procedures were approved by the Animal Ethics Committee of National Institute of Environmental Health Sciences.

Real-time PCR

Mouse liver cDNAs were prepared using High Capacity cDNA Archive Kit (Applied Biosystems) with total RNA prepared with TRIZOL reagent (Invitrogen). Real-time PCR was performed with 7900HT Fast Real-Time PCR System (Applied Biosystems) with the following probes and primers: 5'-6FAM-ACCCTAGACACCACTGGCCGCATGT-TAMR A-3', 5'-CCCTGGGCATGATTGCAA-3', 5'-AAGAGGACGCCACTCACGAT-3' for *Cpt1a*; 5'-6FAM-CATCACGGCCAATGTTATCTGCTCCA-TAMRA-3', 5'-ACCCACGTTCTCTTCCA-3', 5'-CAGCAGGCGCAAGAACTGA-3' for *Cyp2b10* (34). In addition, the following pre-synthesized probes from Applied Biosystems were used: *Cyp3a11*, Mm00731567_m1; *Foxa2*, Mm00839704_mH; *Hmgcs2*, Mm00550050_ml; *Srebp1*, Mm00550338_ml; *Fasn*, Mm00662319_m1; *Acc1*, Mm01304260_m1; *Scd1*, Mm00772290_ml; *Mtp*, Mm01321412_g1; *Dgat2*, Mm00499530_m1; *Cpt2*, Mm00432403_01, *Ppara*; Mm00440939_m1. The TaqMAN rodent GAPDH control reagent (Applied Biosystems) was used as internal control.

Chromatin Immunoprecipitation (ChIP)

ChIP assays were performed according to the method previously reported (35) with some modifications. The liver nuclei were prepared according to previously reported method (36). Nuclear pellets were suspended with PBS containing 3 mM MgCl₂ and treated with 1.0% formaldehyde at room temperature for 15 min for cross-linking. To quench the reaction, glycine (final 125mM) was added and incubated for 5 min. After wash with PBS containing 3 mM MgCl₂, the nuclei were suspended in lysis buffer (50 mM Tris-HCl, pH 8.1, 1.0% SDS, 10 mM EDTA, 1 mM PMSF and one Complete Protease inhibitor minitab (Roche Diagnostics) per 10 ml) for 10 min on ice, and the nuclear lysate was sonicated to shear chromosomal DNA to a size of average 500 bp. Insoluble material was removed by centrifugation and the soluble supernatant solution (200 μl) was diluted 10-fold with ChIP dilution buffer (50 mM HEPES, pH7.5, 150 mM NaCl, 1 mM EDTA, 1.0% Triton X-100, 0.1% sodium deoxycholate, 0.1% SDS, 1 mM PMSF and one Complete Protease inhibitor minitab per 10 ml). The diluted chromatin was precleared by incubating for 4h with 4 mg sheared salmon sperm DNA, 40 μl of pre-immune serum and 25 μl Protein G-agarose beads saturated with BSA (1 mg/ml). The mixture was spun at 3,000 rpm for 2 min at 4°C, and the supernatant was allowed to bind to either 5 μg of normal goat IgG or anti-FOXA2 antibody (IMGENEX Co.) overnight at 4°C. Immunocomplexes on protein G-agarose were pulled down and washed 4 times with the ChIP dilution buffer. DNA precipitated in the anti-FOXA2 antibody complex was decrosslinked and eluted by incubating at 65°C for at 6 h, and treated by Proteinase K for 2 h at 42°C. The purified DNAs using Qiaquick DNA purification columns (Qiagen) were used for semi-quantitative PCR analysis using α-³²P-dATP (Amersham Bioscience) with gene-specific primers as followed. 5'-TACAGCCTAGAACCCTGACTGC-3', 5'-CTTTCCTACTGAGGCCAGATAG-3' for *Cpt1a* promoter, 5'-TGAGCCACTCAGCAGGAATCAG-3', 5'-CTGGGTTGGGCTTTATAAGACTCC-3' for *Hmgcs2* promoter.

Serum and liver parameters analysis

Blood samples were collected from the submandibular cheek-pouch area of mice, using 5.5mm Golden Rod animal lancets (Medipoint, Inc.) and micotainer Serum Separator Tube (Becton Dickinson). The serum levels of triglyceride, non-esterified fatty acid (NEFA) free fatty acid and 3-hydroxybutyrate were measured using assay kits (L-type TG H, NEFA C and Autokit 3-HB, respectively) from Wako chemicals USA, Inc. Serum glucose and cholesterol were measured using reagents and controls from Olympus America Inc. and the chemistry-immuno AU400e analyzer (Olympus). Serum levels of insulin and glucagon were quantified using RIA kits for these hormone from Linco Research, Inc. Total liver lipids were extracted from homogenate prepared from 100 mg liver using methanol-chloroform (1:2 v/v) according to Bligh and Dyer's method (37). After centrifugation, the chloroform fraction was collected and dried. The remaining pellet was dissolved in 10% SDS in isopropanol and triglyceride was assayed using L-type TG H (Wako Chemicals USA, Inc).

Statistical analysis

Statistical analysis was performed by Student's t-test for the drug responses in $Pxr^{+/+}$ mice or $Pxr^{-/-}$ mice and the differences between $Pxr^{+/+}$ mice and $Pxr^{-/-}$ mice.

Results

Regulation of the *Cpt1a*, *Hmgcs2* and *Scd1* genes

First, we have measured the expression of *Cpt1a* and *Hmgcs2*, which are known to be regulated by FoxA2, in mouse liver. Consistent with previous reports (23,24), expression of *Cpt1a* and *Hmgcs2* were induced (3.5 and 2.5 folds, respectively) by 24 hr fasting in mouse livers, apparently through insulin-Akt-FoxA2 pathway regulation (Fig. 1). Interestingly, roughly 40% of the induction was compromised by PCN treatment. Hence, to find PXR roles in the xenobiotics dependent suppression of *Cpt1a* and *Hmgcs2* genes in mouse liver, we compared the expressions of the genes between $Pxr^{+/+}$ and $Pxr^{-/-}$ after PCN treatment in fasting condition (Fig. 2). Only in $Pxr^{+/+}$ mice, PCN treatment repressed *Cpt1a* (35%) and *Hmgcs2* (45%) mRNA expression significantly. In contrast, the same treatment increased mRNA for *Scd1* (4 fold) in fasting $Pxr^{+/+}$ mice (Fig. 2). The down-regulation of the *Cpt1a* and *Hmgcs2* genes and the up-regulation of the *Scd1* gene were not observed in the PCN-treated $Pxr^{-/-}$ mice, indicating these PCN-induced regulations were PXR-dependent. As expected, treatment with PCN induced *Cyp3A11* mRNA more than 10-fold only in WT mice, providing the excellent control of the function of PXR and its activation by PCN in the animal model used (Fig. 2). Since these three genes are hormonally regulated, we measured serum insulin and also glucagon and confirmed that PCN treatment did not change their levels (Table 1). Thus, these results clearly indicated that PXR directly down-regulated *Cpt1a* and *Hmgcs2* genes and up-regulated the *Scd1* gene. We also examined the effect of PCN treatment on PPAR α that regulates the *Cpt1a* and *Hmgcs2* genes and found that PCN did not change the levels of PPAR α mRNA in the $Pxr^{+/+}$ and $Pxr^{-/-}$ mice (data not shown). Several genes involved in lipid metabolism (*Cpt2*, *Srebp1*, *Fasn*, *Acc1*, *Mttp*, and *Dgat2*) were analyzed (Table 2). None of these genes except *Cpt2* and *Srebp1*, which are weakly down-regulated in PCN treated $Pxr^{+/+}$ mice and weakly up-regulated in $Pxr^{-/-}$ mice, respectively, has differential expression in the treatment groups.

Unexpectedly, the serum levels of insulin were found to be 2-fold higher in the $Pxr^{-/-}$ mice compared with these in the $Pxr^{+/+}$ mice (Table 1). This higher level of insulin might have caused the expressions of the *Cpt1a* and *Hmgcs2* genes attenuated and of the *Scd1* gene augmented in the non-treated $Pxr^{-/-}$ mice (Fig. 2). Whether the lack of PXR is directly responsible for this higher insulin levels remained unsolved, since it is still possible at the present time that the mouse with this phenotype happened to be selected during production of this line of $Pxr^{-/-}$ mice.

Repression of the trans-activation activity of FoxA2

To explore molecular mechanism underlying the *Cpt1a* and *Hmgcs2* regulation seen in Fig. 1 and 2, the functional interaction between mPXR and FoxA2 was analyzed in a transient reporter assay using *Cpt1a* and *Hmgcs2* reporters. For the purpose, we cloned mouse *Cpt1a* gene promoters (-2.4k to +1) into a luciferase reporter plasmid and co-transfected the reporter with the expression plasmids for FoxA2 and mPXR into Huh7 cells (Fig. 3A). FoxA2 activated the *Cpt1a* reporters over 20-fold compared with control vector and mPXR repressed this FoxA2-dependent *trans*-activation with more than 80 % repression in the presence of PCN and RXR. In the absence of FoxA2 co-expressed, mPXR did not affect the activity of *Cpt1a* promoter. Thus, the results suggest mPXR needs to be activated to repress the FoxA2 *trans*-activation. Next, we identified FoxA2 binding sites in the promoter of the genes. The results using serial deletion mutants of the reporter constructs suggested FoxA2 binding sites located between -2.1k and -1.6 k in *Cpt1a* gene (Fig. 3B). To further establish the FoxA2 binding sites, candidate binding sequences (C1, C2, and C3 shown in Fig. 3) that have similarity with consensus FoxA2 binding sites were analyzed by gel shift assay and reporter assays using deletion mutants. FoxA2 interacted with both C1 and C3 sites but not C2 site in gel shift analysis (Fig. 3C). C1 and C3 deletion from the -2.4 k reporter diminished more than 70% of FoxA2 activation (Fig 3D).

Similar experiments using *Hmgcs2* reporters suggest activated mPXR also attenuates FoxA2 activation of this gene (Fig. 4). The *Hmgcs2* reporter (-3.0k to +40) was constructed and co-transfected with mPXR and hRXR (Fig. 4A). FoxA2 activated the *Hmgcs2* reporters around 4-fold and mPXR inhibited this *trans*-activation in the presence of PCN. Using similar strategy as shown Fig. 3, we identified FoxA2 binding site in this gene and named H2 site (-112- -98) (Figs. 4B, 4C and 4D). In the absence of exogenous FoxA2 co-expressed, PXR repressed the constitutive activity of *Hmgcs2* reporter activity (Fig. 4A). It is not known whether this constitutive activity was regulated by the endogenous FoxA2 or the other transcription factor. Taken together, the results clearly established that *Cpt1a* and *Hmgcs2* promoters have FoxA2 binding sites and activated mPXR represses FoxA2 dependent *trans*-activation in transient reporter assay using -2.4k *Cpt1a* reporter and -3.0k *Hmgcs2* reporter.

Binding of PXRLBD to FoxA2DBD

To explore the molecular mechanism for the repression of FoxA2 by mPXR, we analyzed interaction of mPXR with FoxA2 in mammalian two-hybrid assay. The reporter activity was increased around 2.5 fold by PCN when GAL4-PXR (pBind/mPXR) was cotransfected with VP16-FoxA2 (pAct/FoxA2, Fig. 5A). However, no PCN effect was observed when only one of these was co-expressed with empty vectors. Since the activation was not seen without the PXR ligand, these results imply mPXR could interact with FoxA2 only when the receptor was activated by PCN.

GST-Pull down assay was performed to determine which regions are required for the interaction between mPXR and FoxA2. We generated GST fusion proteins for full-length FoxA2 and its three deletion mutants, which have a transcriptional activation domain (FoxA2 7-94), the winged-helix DNA binding domain (144-279), or C-terminal region (361-458, Fig. 5B). These GST fusion proteins were purified from bacteria extracts and pull down assay was performed with ³⁵S-labeled *in vitro* translated mPXR. Consistent with the mammalian two hybrid assay results, FoxA2 interacted with mPXR strongly. Furthermore, the winged-helix DNA binding domain showed high affinity with mPXR while N- and C-terminus regions did not. Next, to identify regions in PXR required for the interaction with FoxA2, GST-pull down assays were performed using a set of deletion mutants of mPXR (Fig. 5B). Ligand binding domain (LBD) of mPXR showed strong affinity with GST-FoxA2 fusion protein but the DNA binding domain did not. Interestingly, Δ AF2 still possessed the high affinities with GST-FoxA2

fusion protein, suggesting that AF2 domain is not necessary for the interaction between FoxA2 and the receptors. To provide the additional evidence supporting the binding of the LBD with FoxA2, transient transfection assays using the -2.4k *Cpt1a* reporter were performed. The LBD of mPXR, but not the DBD repressed the reporter activity (Fig. 5C). Collectively these results strongly suggested that mPXR LBD directly interact with FoxA2 winged-helix DNA binding domain *in vitro*.

Inhibition of FoxA2 binding to the promoters

The results showing mPXR bind to the winged-helix DNA binding domain of FoxA2 (Fig. 5B and 5C) suggest possible inhibition of FoxA2 DNA binding by mPXR. Thus, we examined FoxA2 DNA binding activity using gel shift assay in the presence or absence mPXR. Incubating *in vitro* translated FoxA2 with an established FoxA2 binding site probe, one major shifted band was observed (Fig.5D). The shifted band was disappeared in the presence of excess cold competitor. Neither hRXR nor mPXR alone inhibited FoxA2/DNA complex significantly. In contrast, by co-incubating mPXR with hRXR, the shifted band was dramatically decreased. Thus mPXR and RXR heterodimer could inhibit FoxA2 DNA binding. To establish this inhibition is occurring in liver *in vivo*, we did ChIP analysis using mouse liver extracts from *Pxr*^{+/+} and *Pxr*^{-/-} mice treated with PCN. If the repression of *Cpt1a* and *Hmgcs2* by PXR was due to inhibition of FoxA2 recruitment to the cis-elements, ChIP assay could detect the FoxA2 occupancy change at the promoter sites for the genes by PCN treatment. FoxA2 responsible elements on *Cpt1a* and *Hmgcs2* promoter determined in Figs. 3 and 4 were amplified from immunoprecipitated material using anti-FoxA2 from mouse liver extracts. As shown in Fig. 5E, both amplified DNA fragments of the *Cpt1a* and *Hmgcs2* genes were decreased only in *Pxr*^{+/+} mice treated with PCN but not in *Pxr*^{-/-} mice. Semi quantification of the band intensities from multiple ChIP assays suggested that PCN treatment decreased the FoxA2 occupations on the *Cpt1a* and *Hmgcs2* promoters by 60 ± 27% and 30 ± 16%, respectively. Taken together, with the earlier results these data suggested inhibition of FoxA2 DNA binding on *Cpt1a* and *Hmgcs2* promoters by the direct interaction between activated PXR and FoxA2 in nucleus.

Liver and serum parameters

The gene regulation difference we found in the previous experiments might be reflected in blood and/or hepatic lipid content differences caused by PCN treatment. Therefore, we analyzed blood chemistry and hepatic triglyceride content (Table 3 and Fig. 6A) of PCN treated or untreated *Pxr*^{+/+} and *Pxr*^{-/-} mice in fasting condition. Serum glucose and ketone body (3-hydroxybutylate) levels were significantly decreased in *Pxr*^{+/+} mice treated with PCN (Table 3). Moreover the treatment increased hepatic triglyceride quantity only in WT mice livers nearly two fold (Fig. 6A), while serum triglyceride and NEFA amounts were not affected (Table 3). Consistent with the hepatic triglyceride increase, a remarkable multiplication of microvesicular lipid droplets was observed panlobularly in PCN treated WT mice liver sections (Fig. 6B).

Surprisingly, hepatic triglyceride contents in *Pxr*^{-/-} mice were much higher than those of *Pxr*^{+/+} mice (about 2 fold). Furthermore, lipid staining of the sections from these mice showed dramatic difference from those in WT sections. As shown in figure 6B, *Pxr*^{-/-} mice had macrovesicular lipid droplets dominantly localized in centrilobular areas. In addition, panlobular microvesicular droplets were also increased significantly compare to WT untreated mice livers. As expected, PCN treatment gave no significant change either in blood chemistry, in hepatic triglyceride, or in lipid staining in *Pxr*^{-/-} mice livers. Collectively, these results suggest that PXR plays critical roles in lipid metabolism/synthesis in fasting mouse liver and the gene expression changes we found in Fig. 1 (*Cpt1a*, *Hmgcs2* and *Scd1*) may explain at least partially these physiological changes in mice.

Discussion

We have demonstrated that activation of PXR up-regulates the *Scd1* gene and down-regulates the *Cpt1a* and *Hmgsc2* genes in the liver of fasting mice. Concomitantly, the level of hepatic triglycerides is increased and that of serum 3-hydroxybutyrate decreased. Thus, activated PXR represses hepatic energy metabolism by increasing triglyceride synthesis and decreasing β -oxidation and ketogenesis in the fasting mice (Fig. 7). This regulation by PXR is similar to that by insulin, which also increases the level of SCD1 and decreases that of CPT1A and HMGCS2 (23,24,38,39). PXR represses the FoxA2-mediated transcription of the *Cpt1a* and *Hmgsc2* genes by directly binding to FoxA2, which differs from insulin that indirectly represses this transcription by activating the Akt-dependent signal pathway (25). Thus, PXR can repress hepatic energy metabolism in an insulin-independent manner, providing the basis for future investigations to understand and treat insulin-insensitive liver diseases.

The *Cpt1a* promoter contains the two FoxA-binding sequences in the distal region (-1910/-1886 and -1733/-1719), while the *Hmgsc2* promoter bears the one active sequence in the proximal region (-176/-182). Deletion of these sequences abrogated the FoxA2-mediated transcription of these promoters. Through its LBD, PXR directly binds to the DBD (residues 144/279) of FoxA2 and prevents the FoxA2 binding to its response sequences of the promoters, repressing the transcription of the *Cpt1a* and *Hmgsc2* gene. PXR and also CAR are known to repress another insulin response transcription factor FoxO1 that plays the major role in the regulation of hepatic gluconeogenesis (17). Mechanistically resembling the repression of FoxA2 activity, PXR directly binds to FoxO1 and down-regulates the FoxO1-mediated transcription of the *Pepck1* gene. In fact, it has recently been reported the *Pepck1* and *G6Pase* genes are up-regulated in the transgenic mice expressing constitutively activated PXR (40). Thus, the xenobiotic sensing nuclear receptors make use of a similar molecular mechanism to repress gluconeogenesis, β -oxidation and ketogenesis through direct binding to members of the forkhead transcription factor family FoxO1 and FoxA2.

The rate-limiting enzymes FAS and ACC1 in fatty acid synthesis were not regulated by PXR. Therefore, the hepatic level of triglycerides does not seem to be due to an increase of fatty acid synthesis in the liver. In addition to SCD1, the other enzymes DGAT2 and MTTP involved in triglyceride synthesis and secretion were examined and found not to be regulated by PXR. Thus, SCD1 is the major enzyme responsible for the hepatic accumulation of triglycerides and lipid droplets in the present animal model. The *Scd1* gene was up-regulated in the transgenic mouse bearing the constitutively activated PXR (40). SCD1 has long been known to play the key role in triglyceride synthesis: the *Scd1* null mice have a lower level of triglyceride in the liver than *Scd1* wild type mice and over-expressing SCD1 in CHO cells elevated the cellular level of triglycerides (41,42). The molecular mechanism of PXR-mediated activation of the *Scd1* gene remains uninvestigated at the present time (Fig. 7). Insulin treatment also up-regulates the *Scd1* gene, in which insulin activates the SREBP-SRE mediated transcription (43). Whether or not PXR cross talks with the SREBP signal pathway to up-regulate the *Scd1* gene will be an interesting question for future investigations. The down-regulation of *Cpt1a* by PXR may also have had additionally contributed to the increase of hepatic triglycerides in the PCN-treated mice. It has been shown that treating mice with the CPT1A inhibitor tetradecylglycidic acid elevated hepatic triglycerides (44). Moreover, the heterozygous *Cpt1a*-null mouse exhibited an elevated level of serum triglycerides (45). By up-regulating and down-regulating SCD1 and CPT1A, respectively, drug activation of PXR can effectively lead the liver to develop steatosis.

The serum glucose level in the fasting *Pxr*^{+/+} mouse was reduced by PCN treatment, indicating that the activated PXR mediates the drug-induced decrease of serum glucose. As previously shown, PXR can directly down-regulate FoxO1-mediated transcription, thus repressing

gluconeogenesis (17). Given the finding that PXR down-regulates the *Cpt1a* gene, xenobiotics and drugs such as PCN that activate PXR may also repress gluconeogenesis by down-regulating the genes such as *Cpt1a* and β -oxidation. Since β -oxidation produces chemical energy and reducing agents such as ATP and NADH, its decline limits the supply of these chemicals required for gluconeogenesis to proceed. With the simultaneous decreases of both glucose and ketone bodies, the PCN-treated mice develop a similar phenotype to the hypoketotic hypoglycemia observed in *CPT1A*- or *HMGCS2*-deficient patients (46,47), and thus provide us with an animal model to investigate the relevant human diseases.

A most intriguing finding from our present study was the fact that the untreated *Pxr*^{-/-} mice developed severe steatoses, as indicated by the accumulation of triglycerides and large lipid droplets in the liver. Consistently, the *Scd1* and *Cpt1a* gene were up- and down-regulated, respectively in the liver of these mice. The *Hmgcs2* gene was also constitutively down-regulated and the serum level of 3-hydroxybutyrate was decreased in *Pxr*^{-/-} mice. The phenotypes observed in the *Pxr*^{-/-} mouse appear to be comparable to those observed in the PCN-treated *Pxr*^{+/+} mice; both the activation and lack of PXR regulate these genes similarly, resulting in the development of steatosis. These phenotypes were correlated with the high levels of serum insulin in the *Pxr*^{-/-} mice. Although it remains further investigated, there is the possibility that the endogenous PXR (PXR not activated by drugs) is capable of protecting insulin to elevate its serum levels, thus preventing the liver from developing steatosis and to control ketogenesis. The mechanism of how endogenous PXR regulates serum insulin levels is beyond speculation at the present time. In conclusion, drug-activated PXR is capable of increasing lipogenesis in the liver and of decreasing hepatic β -oxidation and ketogenesis by regulating the genes encoding the key enzymes that catalyze these hepatic metabolic pathways (Fig. 7). The PXR, in part, regulates these genes through cross-talk with the insulin response transcription factor FoxA2, functionally mimicking the effect of insulin. Endogenous PXR also regulates the same set of genes that are regulated by the drug-activated PXR, for which the molecular mechanism is not known. If, in fact, the endogenous PXR is to regulate serum insulin levels, considering the repressive role of the endogenous PXR in the development of steatoses in the untreated *Pxr*^{+/+} mice, we are urged to identify the ligand and/or signal pathway that regulate this function of endogenous PXR.

Acknowledgements

This research was supported by the Intramural Research Program of the NIH, National Institute of Environmental Health Sciences.

References

1. Honkakoski P, Zelko I, Sueyoshi T, Negishi M. Mol Cell Biol 1998;18(10):5652–5658. [PubMed: 9742082]
2. Sueyoshi T, Kawamoto T, Zelko I, Honkakoski P, Negishi M. J Biol Chem 1999;274(10):6043–6046. [PubMed: 10037683]
3. Kliewer SA, Moore JT, Wade L, Staudinger JL, Watson MA, Jones SA, McKee DD, Oliver BB, Willson TM, Zetterstrom RH, Perlmann T, Lehmann JM. Cell 1998;92(1):73–82. [PubMed: 9489701]
4. Honkakoski P, Sueyoshi T, Negishi M. Ann Med 2003;35(3):172–182. [PubMed: 12822739]
5. Willson TM, Kliewer SA. Nat Rev Drug Discov 2002;1(4):259–266. [PubMed: 12120277]
6. Yamamoto Y, Kawamoto T, Negishi M. Arch Biochem Biophys 2003;409(1):207–211. [PubMed: 12464260]
7. Sonoda J, Rosenfeld JM, Xu L, Evans RM, Xie W. Curr Drug Metab 2003;4(1):59–72. [PubMed: 12570746]
8. Wei P, Zhang J, Egan-Hafley M, Liang S, Moore DD. Nature 2000;407(6806):920–923. [PubMed: 11057673]
9. Sueyoshi T, Negishi M. Annu Rev Pharmacol Toxicol 2001;41:123–143. [PubMed: 11264453]

10. Goodwin B, Redinbo MR, Kliever SA. *Annu Rev Pharmacol Toxicol* 2002;42:1–23. [PubMed: 11807162]
11. Sugatani J, Kojima H, Ueda A, Kakizaki S, Yoshinari K, Gong QH, Owens IS, Negishi M, Sueyoshi T. *Hepatology* 2001;33(5):1232–1238. [PubMed: 11343253]
12. Sugatani J, Sueyoshi T, Negishi M, Miwa M. *Methods Enzymol* 2005;400:92–104. [PubMed: 16399345]
13. Xie W, Yeuh MF, Radominska-Pandya A, Saini SP, Negishi Y, Bottroff BS, Cabrera GY, Tukey RH, Evans RM. *Proc Natl Acad Sci U S A* 2003;100(7):4150–4155. [PubMed: 12644700]
14. Runge-Morris M, Kocarek TA. *Curr Drug Metab* 2005;6(4):299–307. [PubMed: 16101570]
15. Klaassen CD, Slitt AL. *Curr Drug Metab* 2005;6(4):309–328. [PubMed: 16101571]
16. Ueda A, Hamadeh HK, Webb HK, Yamamoto Y, Sueyoshi T, Afshari CA, Lehmann JM, Negishi M. *Mol Pharmacol* 2002;61(1):1–6. [PubMed: 11752199]
17. Kodama S, Koike C, Negishi M, Yamamoto Y. *Mol Cell Biol* 2004;24(18):7931–7940. [PubMed: 15340055]
18. Rosenfeld JM, Vargas R Jr, Xie W, Evans RM. *Mol Endocrinol* 2003;17(7):1268–1282. [PubMed: 12663745]
19. Bartlett K, Eaton S. *Eur J Biochem* 2004;271(3):462–469. [PubMed: 14728673]
20. Laffel L. *Diabetes Metab Res Rev* 1999;15(6):412–426. [PubMed: 10634967]
21. Fukao T, Lopaschuk GD, Mitchell GA. *Prostaglandins Leukot Essent Fatty Acids* 2004;70(3):243–251. [PubMed: 14769483]
22. Eaton S, Bartlett K, Pourfarzam M. *Biochem J* 1996;320(Pt 2):345–357. [PubMed: 8973539]
23. Hegardt FG. *Biochem J* 1999;338(Pt 3):569–582. [PubMed: 10051425]
24. Louet JF, Le May C, Pegorier JP, Decaux JF, Girard J. *Biochem Soc Trans* 2001;29(Pt 2):310–316. [PubMed: 11356173]
25. Wolfrum C, Asilmaz E, Luca E, Friedman JM, Stoffel M. *Nature* 2004;432(7020):1027–1032. [PubMed: 15616563]
26. Wolfrum C, Besser D, Luca E, Stoffel M. *Proc Natl Acad Sci U S A* 2003;100(20):11624–11629. [PubMed: 14500912]
27. Wang H, Wollheim CB. *Trends Mol Med* 2005;11(6):262–265. [PubMed: 15949766]
28. Kiyosawa N, Tanaka K, Hirao J, Ito K, Niino N, Sakuma K, Kanbori M, Yamoto T, Manabe S, Matsunuma N. *Arch Toxicol* 2004;78(8):435–442. [PubMed: 15107969]
29. Rausa FM, Tan Y, Costa RH. *Mol Cell Biol* 2003;23(2):437–449. [PubMed: 12509444]
30. Pani L, Overdier DG, Porcella A, Qian X, Lai E, Costa RH. *Mol Cell Biol* 1992;12(9):3723–3732. [PubMed: 1324404]
31. Squires EJ, Sueyoshi T, Negishi M. *J Biol Chem* 2004;279(47):49307–49314. [PubMed: 15347657]
32. Kobayashi K, Sueyoshi T, Inoue K, Moore R, Negishi M. *Mol Pharmacol* 2003;64(5):1069–1075. [PubMed: 14573755]
33. Allander SV, Durham SK, Scheimann AO, Wasserman RM, Suwanichkul A, Powell DR. *Endocrinology* 1997;138(10):4291–4300. [PubMed: 9322942]
34. Kakizaki S, Karami S, Negishi M. *Drug Metab Dispos* 2002;30(2):208–211. [PubMed: 11792692]
35. Ishii S, Iizuka K, Miller BC, Uyeda K. *Proc Natl Acad Sci U S A* 2004;101(44):15597–15602. [PubMed: 15496471]
36. Gorski K, Carneiro M, Schibler U. *Cell* 1986;47(5):767–776. [PubMed: 3779841]
37. Bligh EG, Dyer WJ. *Can J Biochem Physiol* 1959;37(8):911–917. [PubMed: 13671378]
38. Waters KM, Ntambi JM. *J Biol Chem* 1994;269(44):27773–27777. [PubMed: 7961698]
39. Mounier C, Posner BI. *Can J Physiol Pharmacol* 2006;84(7):713–724. [PubMed: 16998535]
40. Zhou J, Zhai Y, Mu Y, Gong H, Uppal H, Toma D, Ren S, Evans RM, Xie W. *J Biol Chem* 2006;281(21):15013–15020. [PubMed: 16556603]
41. Listenberger LL, Han X, Lewis SE, Cases S, Farese RV Jr, Ory DS, Schaffer JE. *Proc Natl Acad Sci U S A* 2003;100(6):3077–3082. [PubMed: 12629214]
42. Miyazaki M, Kim YC, Gray-Keller MP, Attie AD, Ntambi JM. *J Biol Chem* 2000;275(39):30132–30138. [PubMed: 10899171]

43. Tabor DE, Kim JB, Spiegelman BM, Edwards PA. *J Biol Chem* 1999;274(29):20603–20610. [PubMed: 10400691]
44. Grefhorst A, Hoekstra J, Derks TG, Ouwens DM, Baller JF, Havinga R, Havekes LM, Romijn JA, Kuipers F. *Am J Physiol Gastrointest Liver Physiol* 2005;289(3):G592–598. [PubMed: 15817811]
45. Nyman LR, Cox KB, Hoppel CL, Kerner J, Barnoski BL, Hamm DA, Tian L, Schoeb TR, Wood PA. *Mol Genet Metab* 2005;86(12):179–187. [PubMed: 16169268]
46. Olpin SE. *Prostaglandins Leukot Essent Fatty Acids* 2004;70(3):293–308. [PubMed: 14769488]
47. Rinaldo P, Matern D, Bennett MJ. *Annu Rev Physiol* 2002;64:477–502. [PubMed: 11826276]

The abbreviations used are

CAR	constitutive active/androstane receptor
PXR	Pregnane X receptor
PB	Phenobarbital
RXR	retinoid X receptor
FoxA2	forkhead box A2
CPT1A	carnitine palmitoyltransferase 1
HMGCS2	mitochondrial 3-hydroxy-3-methylglutarate CoA synthase 2
PCN	pregnenolone 16 α -carbonitrile
SCD1	stearoyl CoA desaturase 1
PEPCK1	phosphoenolpyruvate carboxykinase 1
G6Pase	glucose-6-phosphatase
DMSO	dimethyl sulfoxide
GST	glutathione S-transferase
DBD	DNA binding domain
LBD	ligand binding domain
AF2	activation function 2

SREBP1	sterol regulatory element-binding protein 1
ACC1	acetyl CoA carboxylase 1
FAS	fatty acid synthase
DGAT2	diglycerol acyltransferase 2
MTTP	microsomal triacylglyceride transfer protein
Akt	protein kinase B
IRS	insulin response sequence
ChIP	Chromatin immunoprecipitation assay
NEFA	non-esterified fatty acids

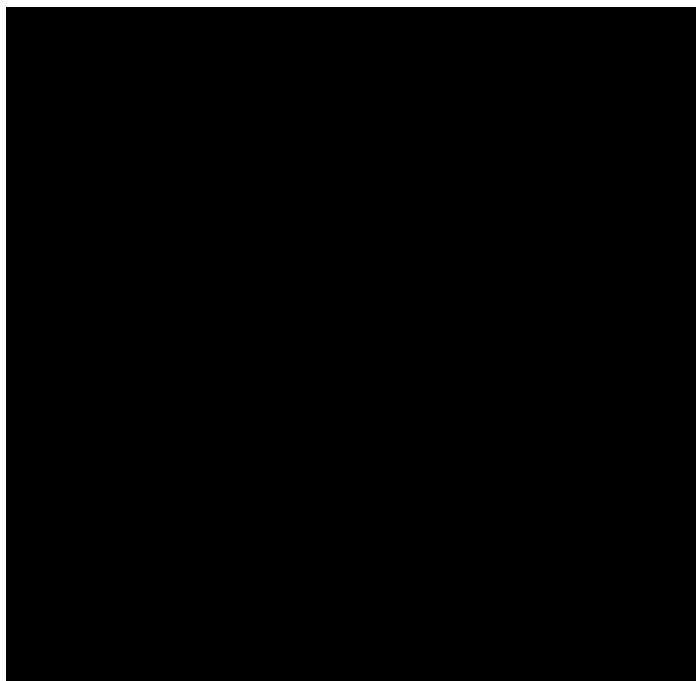


Fig. 1. PCN treatment represses mRNA levels of *Cpt1a* and *Hmgcs2* in fasting mice. Cr1: CD-1 (ICR) BR male mice were intraperitoneally injected with PCN (20 mg/kg of body weight) or DMSO, and were either fed at libitum or fasted with drinking water for 24 hours. The mRNA levels in these mouse livers were determined by real-time RT-PCR and were expressed by taking those in the fed mice treated with DMSO as one. Values express mean \pm standard deviations (n=4). *p<0.005 for vehicle injected fasted group vs PCN injected fasted group. # p<0.005 for vehicle injected fed group vs PCN injected fed group.

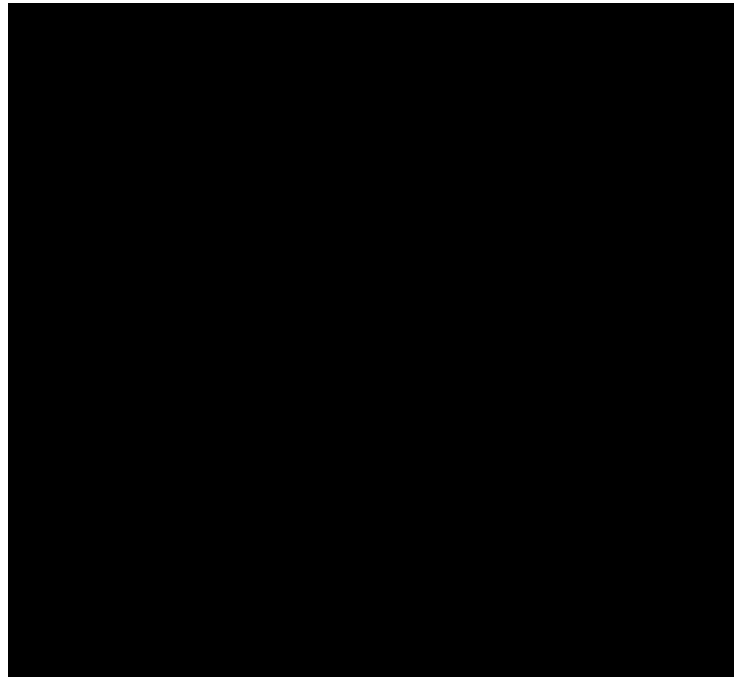


Fig. 2. PXR diversely regulates gene expressions of *Cpt1a*, *Hmgcs2* and *Scd1* in fasting mouse liver. *Pxr*^{+/+} (+/+) or *Pxr*^{-/-} (-/-) mice were treated by intraperitoneal injection with PCN or vehicle (DMSO). The mice were fasted for 24 hours after the injection. *Cpt1a*, *Hmgcs2*, *Scd1* and *Cyp3a11* mRNA levels in these mice liver were determined by real-time RT-PCR. Relative mRNA quantity for each gene was expressed by taking those with DMSO as one. Values express mean \pm standard deviations. *p< 0.005 for vehicle injected *Pxr*^{+/+} group vs PCN injected *Pxr*^{+/+} group. #p<0.005 for vehicle injected *Pxr*^{+/+} group vs vehicle injected *Pxr*^{-/-} group.

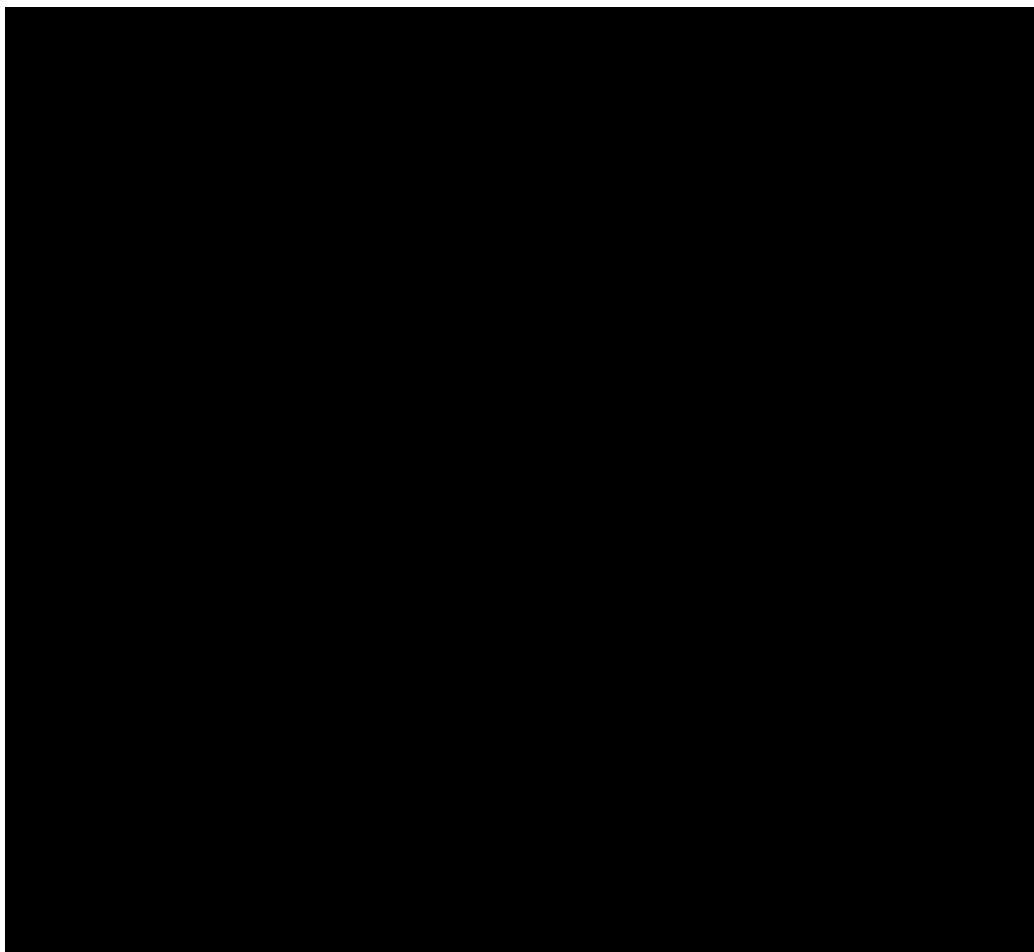


Fig. 3. PXR represses FoxA2 trans-activation of the mouse *Cpt1a* promoter in Huh7 cells. **A.** Reporter plasmid, pGL3/CPT1A -2.4k was co-transfected with or without FoxA2 in the presence or absence of mPXR and hRXR as indicated. At 24 h after the transfection, cells were treated with DMSO or PCN and incubated for additional 24 h. Relative luciferase activities were calculated by taking the activity of the DMSO treated cells transfected with the reporter plasmid alone as one. **B.** A series of pGL3/CPT1A reporter plasmids as indicated were co-transfected with or without FoxA2 for 48 h. Numbers on the vertical axis indicate lengths of the *Cpt1a* promoter cloned into the reporter plasmids. Relative luciferase activities were calculated by taking the activity of the cells transfected with the pGL3/CPT1A -2.4k without FoxA2 as one. **C.** *In vitro*-translated FoxA2 was incubated with ³²P-labeled double-stranded putative FoxA2 binding sites, C1, C2 and C3 within the *Cpt1a* promoter and FoxA2 binding site of IGF1BP-1 promoter. Cold probes stand for the one hundred-fold molar excess competitor co-incubation. Shifted bands were separated by electrophoresis on a 4% polyacrilamide gel. Bands were detected by autoradiography. **D.** Reporter plasmid, pGL3/CPT1A -2.4k and the deletion mutants of the putative FoxA2 binding sites, C1 and C3, were co-transfected with or without FoxA2 for 48 h. Relative luciferase activities were calculated by taking the activity of the cells transfected with the pGL3/CPT1A -2.4k without FoxA2 as one. Bars indicate mean \pm standard deviations in A, B, and D.

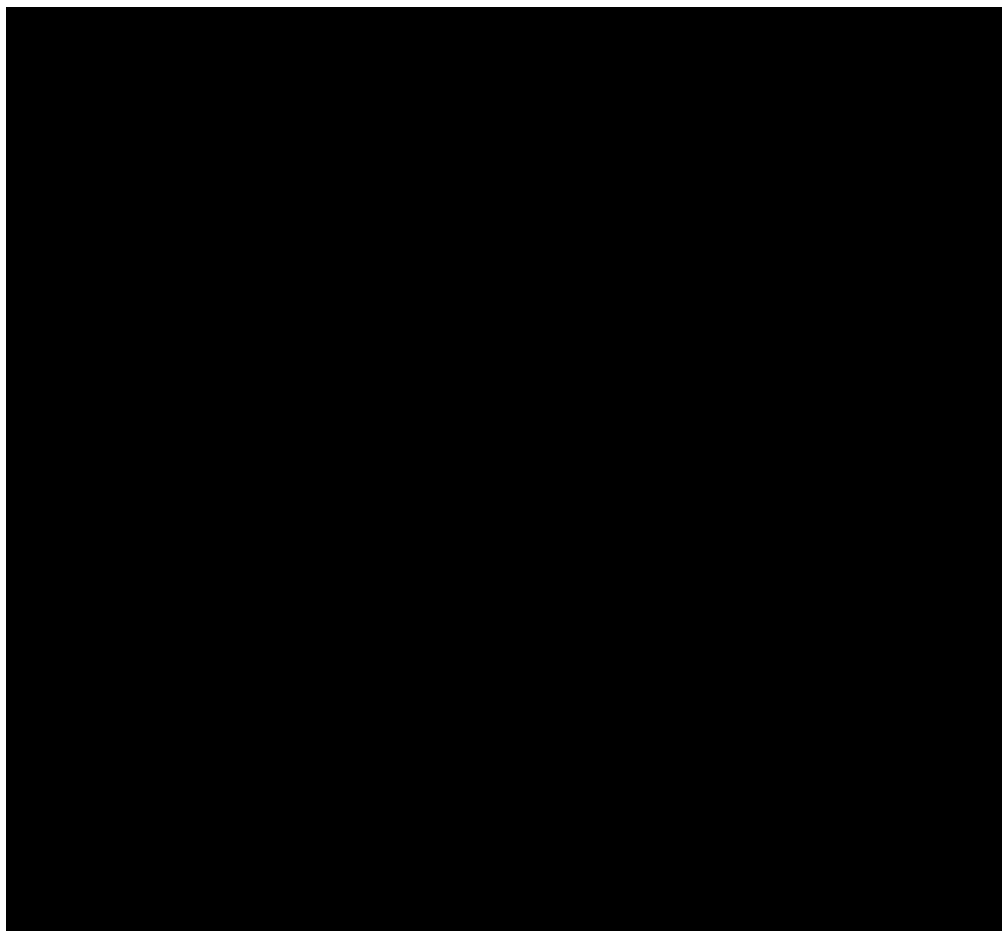


Fig. 4. PXR represses FoxA2 trans-activation of the mouse *Hmgcs2* promoter in Huh7 cells. A. Reporter plasmid, pGL3/HMGCS2 -3.0k was co-transfected with or without FoxA2 in the presence or absence of mPXR and hRXR as indicated. Cell treatments and data analyses were done as in Fig 2A. A series of pGL3/HMGCS2 reporter plasmids as indicated were co-transfected with or without FoxA2 for 48 h. Numbers on the vertical axis indicate lengths of the *Hmgcs2* promoter cloned into the reporter plasmids. Relative luciferase activities were calculated by taking the activity of the cells transfected with the pGL3/HMGCS2 -3.0k without FoxA2 as one. C. *In vitro*-translated FoxA2 was incubated with ³²P-labeled double-stranded putative FoxA2 binding sites, H1 and H2 within the *Hmgcs2* promoter and a FoxA2 binding site of IGFBP-1 promoter. Gel shift analyses were performed as in Fig 2C. D. Reporter plasmid, pGL3/HMGCS2 -3.0k and the deletion mutants of the putative FoxA2 binding sites, H1 and H2, were co-transfected with or without FoxA2 for 48 h. Relative luciferase activities were calculated by taking the activity of the cells transfected with the pGL3/HMGCS2 -3.0k without FoxA2 as one. Bars indicate mean \pm standard deviations in A, B, and D.

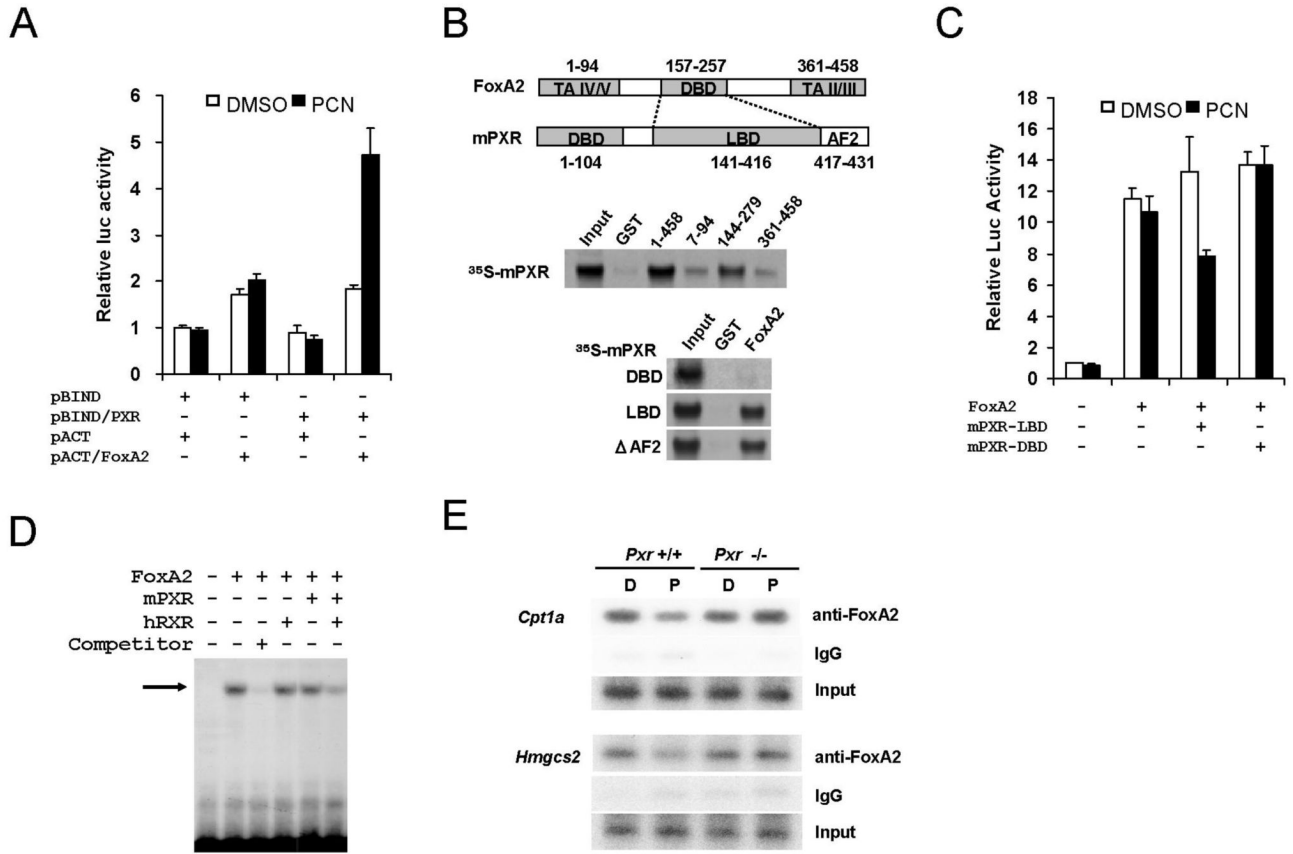


Fig. 5. PXR directly interacts with the DBD of FoxA2 to inhibit its binding to the responsible elements *in vitro* and *in vivo*. **A.** Mammalian two-hybrid assay was performed by co-transfecting pG5-Luc reporter plasmid with various combinations of pBIND, pACT, pBIND/mPXR and pACT/FoxA2 into HepG2 cells. At 24 h after transfection, cells were treated with DMSO or PCN for an additional 24 h. Relative luciferase activities were calculated by taking the activity obtained from the GAL4DBD- and VP16AD-transfected cells in the presence of DMSO as one. Bars indicate mean \pm standard deviations. **B.** Schematic structure of FoxA2 and mPXR (Upper panel). *In vitro* translated ^{35}S -labeled mPXR was incubated with bacterially expressed GST-FoxA2 and its deletion mutants (middle panel). *In vitro* translated ^{35}S -labeled mPXR or the deletion mutants was incubated with bacterially expressed GST-FoxA2 (lower panel). GST-pull down assay was carried out as in EXPERIMENTAL PROCEDURES. Bound proteins were detected by autoradiography. **C.** PXR LBD represses the FoxA2-mediated activation of mouse *Cpt1a* -2.4k reporter. pGL3/CPT1a -2.4k reporter plasmid and pcDNA3.1/FoxA2 were co-transfected with and without pcDNA3.1/mPXR-LBD-V5-His or pcDNA3.1/mPXR-DBD-V5-His into HepG2 cells. After 24 h, DMSO or PCN was added to the cells cultured for additional 24 h. Relative luciferase activities were calculated by taking the activity of the DMSO-treated cells transfected with pGL3/CPT1a -2.4k reporter plasmid alone as one. **D.** *In vitro*-translated FoxA2, mPXR and hRXR were incubated with ^{32}P -labeled double-stranded FoxA2 binding site of IGF1P-1 promoter. Competitor stands for fifty-fold excess cold probe co-incubation. Shifted bands were separated by electrophoresis on a 4% polyacrilamide gel. Bands were detected by autoradiography. **E.** Activated PXR inhibits FoxA2 binding to *Cpt1a* and *Hmgcs2* promoter in ChIP assay. Chromatin fragments were immunoprecipitated with anti-FoxA2 antibody from liver nuclear extracts. Precipitated *Cpt1a* and *Hmgcs2* promoter DNA

was semi-quantified by PCR as in EXPERIMENTAL PROCEDURES. D and P stands for DMSO and PCN treated mouse liver, respectively.

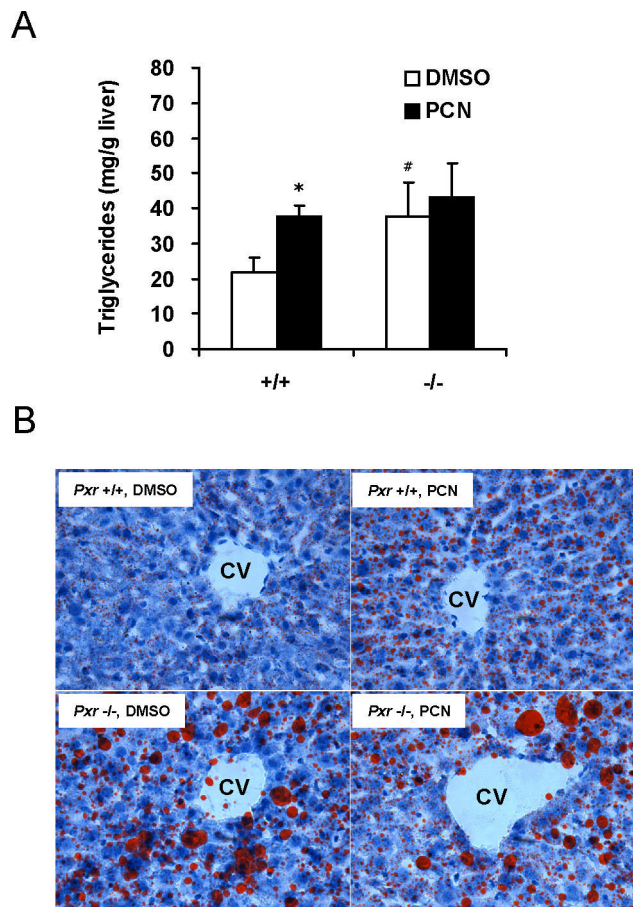


Fig. 6. PXR activation by PCN and disruption of PXR gene accumulates hepatic triglyceride in mice. A. Hepatic triglyceride from *Pxr*^{+/+} (+/+) and *Pxr*^{-/-} (-/-) fasted mice treated with DMSO or PCN (n = 4 for each group) were measured as described in EXPERIMENTAL PROCEDURES. Bars indicate mean \pm standard deviations. *p<0.005 for vehicle injected *Pxr*^{+/+} group vs PCN injected *Pxr*^{+/+} group, #p<0.05 for vehicle injected *Pxr*^{+/+} group vs vehicle injected *Pxr*^{-/-} group. B. Oil-red-O staining for neutral lipids in livers of fasted *Pxr*^{+/+} and *Pxr*^{-/-} mice treated with DMSO or PCN. Magnitude: $\times 200$. CV: central vein.

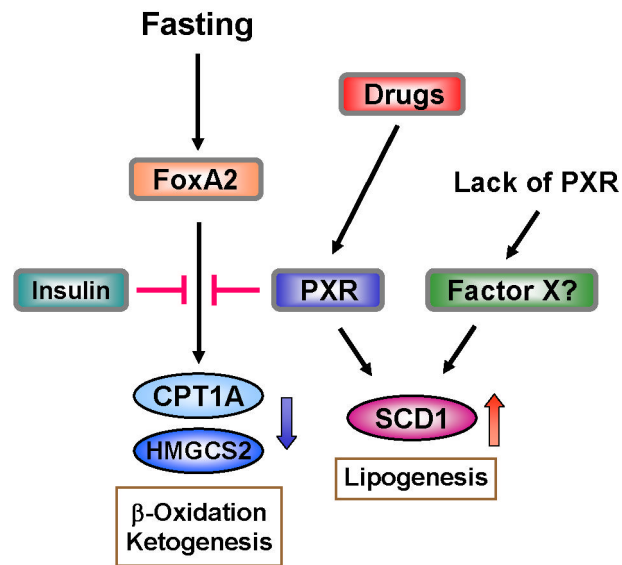


Fig. 7. Schematic representation of cross talk between PXR and FoxA2 for regulation of lipid metabolism. Arrows indicate activation and stop bar indicate repression. Activated PXR represses FoxA2 activity to down regulate gene expressions of CPT1A or HMGCS2 while activating that of SCD1. Regulatory mechanism of SCD1 gene expression by PXR is not known at the present time.

Table 1

Serum levels of insulin and glucagon in wild type and *Pxr*^{-/-} mice

		0hr	12hr	24hr
Insulin (ng/ml)	<i>Pxr</i> ^{+/+}	DMSO	0.24±0.16 ^{**}	0.08±0.04
		PCN	0.21±0.13 [#]	0.09±0.07
	<i>Pxr</i> ^{-/-}	DMSO	0.54±0.24 ^{**}	0.06±0.05
		PCN	0.68±0.34 [#]	0.17±0.12
Glucagon (pg/ml)	<i>Pxr</i> ^{+/+}	DMSO	46.5±13.9	48.8±17.0
		PCN	62.4±30.7	37.5±5.7
	<i>Pxr</i> ^{-/-}	DMSO	59.0±17.2	50.8±12.1
		PCN	60.2±49.2	76.7±16.2

Each value shows mean±SD(n=4).

* P<0.05 for *Pxr*^{+/+} group vs *Pxr*^{-/-} group.** P<0.05 for *Pxr*^{+/+} vehicle treated group vs *Pxr*^{-/-} vehicle treated group.# P<0.05 for *Pxr*^{+/+} PCN treated group vs *Pxr*^{-/-} PCN treated group.

Table 2
Relative mRNA expressions of several key genes involved in lipid homeostasis

Genes	<i>Pxr</i> ^{+/+}		<i>Pxr</i> ^{-/-}	
	DMSO	PCN	DMSO	PCN
Fatty acid synthesis				
<i>Srebp1</i>	100 ±18.5	95.3 ±14.1	172 ±21.8 [#]	158 ±27.8
<i>Fas</i>	100 ±47.5	76.5 ±11.9	84.5 ±19.3	100 ±14.2
<i>Acc1</i>	100 ±38.9	94.2 ±14.3	105 ±14.1	113 ±21.3
TG synthesis and secretion				
<i>Mttp</i>	100 ±10.6	96.6 ±6.2	111 ±13.4	113 ±14.1
<i>Dgat2</i>	100 ±14.2	111 ±12.6	127 ±44.0	120 ±16.8
β-oxidation				
<i>Cpt2</i>	100 ±25.4	78.2 ±11.5	97.7 ±34.7	105 ±23.3

Each value (mean ±SD (n=4)) stands for relative mRNA expression level which was calculated taking that in vehicle injected *Pxr*^{+/+} group as 100 for each gene.

[#] p<0.03 for vehicle injected *Pxr*^{+/+} group vs vehicle injected *Pxr*^{-/-} group.

Blood chemistry

Table 3

Parameter	<i>Pxr</i> +/+		<i>Pxr</i> -/-	
	Control	PCN	Control	PCN
Glucose (mg/dl)	97.5± 10.9	69.3± 18.4*	107± 27.7	88.0± 12.3
Total cholesterol (mg/dl)	127± 23.3	142± 9.5	133± 26.1	149± 24.1
Triglycerides (mg/dl)	50.1± 23.1	65.0± 20.5	44.0± 23.0	52.5± 13.6
NEFA (mEq/l)	1.06± 0.13	1.13± 0.18	1.07± 0.59	1.05± 0.17
3-hydroxybutyrate (mM)	2.10± 0.45	1.17± 0.21**	1.45± 0.55	1.64± 0.27

Each value shows mean ± SD (n=4).

* p<0.05.

** p<0.001 for vehicle injected *Pxr* +/+ group vs PCN injected *Pxr* +/+ group